nanomaterials

MDPI

Communication

Crystallization of Nano-Sized Macromolecules by the Example of Hexakis-[4-{(N-Allylimino)methyl}phenoxy]cyclotriphosphazene

Evgeniy Chistyakov [1,*], Pavel Yudaev [1] and Yulia Nelyubina [2]

[1] Department of Chemical Technology of Polymers, Mendeleev University of Chemical Technology of Russia, Miusskaya Sq., 9, 125047 Moscow, Russia; yudaevpavel5@gmail.com
[2] Center for Molecular Composition Studies, A.N. Nesmeyanov Institute of Organoelement Compounds of Russian Academy of Sciences (INEOS RAS), 28 Vavilov Str., 119334 Moscow, Russia; unelya@ineos.ac.ru
* Correspondence: ewgenij@rambler.ru

Abstract: The synthesized compound was characterized by ^{31}P, ^{13}C, and ^{1}H NMR spectroscopy and MALDI-TOF mass spectroscopy. According to DSC data, the compound was initially crystalline, but the crystal structure was defective. The crystals suitable for X-ray diffraction study were prepared by slow precipitation of the compound from a solution by a vapor of another solvent. A study of the single crystal obtained in this way demonstrated that the phosphazene ring has a flattened chair conformation. It was found that the sphere circumscribed around the compound molecule has a diameter of 2.382 nm.

Keywords: single crystal; crystal structure; nanoparticle; phosphazene; X-ray diffraction

Citation: Chistyakov, E.; Yudaev, P.; Nelyubina, Y. Crystallization of Nano-Sized Macromolecules by the Example of Hexakis-[4-{(N-Allylimino)methyl}phenoxy] cyclotriphosphazene. *Nanomaterials* **2022**, *12*, 2268. https://doi.org/10.3390/nano12132268

Academic Editors: Yangcheng Lu and Zhendong Liu

Received: 9 June 2022
Accepted: 27 June 2022
Published: 30 June 2022

1. Introduction

Azomethines (Schiff bases) are promising compounds for use in various fields of science and technology: extraction of metals [1,2], analytical chemistry [3], chemosensorics [4], polymer photostabilization [5], etc. Azomethines inhibit steel corrosion in hydrochloric [6] and sulfuric [7] acid solutions since they are easily adsorbed at the metal/solution interface. Azomethines with various substituents at nitrogen and carbon atoms are applied in medicine and pharmacology owing to their antimicrobial action, lack of toxicity [8,9], and biological activity [10,11]. Schiff bases with benzothiazole and sulfonate groups inhibit a pancreatic enzyme: lipase; this is important for the treatment of obesity [12]. Polymer hydrogels containing azomethine bonds serve as drug carriers, as they undergo biodegradation via hydrolysis of the CH=N bond [13]. Chitosan linked to a polymeric Schiff base selectively extracts Au(III) and Ag(I) from acidic aqueous solutions (pH = 1) in the presence of divalent heavy metals: copper, lead, cadmium, and zinc [14].

Azomethines are precursors for the synthesis of new compounds with valuable properties. For example, O-phosphorylated derivatives of pyridoxal, a vitamin involved in biochemical processes, were prepared using azomethines [15].

Schiff bases can coordinate transition metals; therefore, they are used to manufacture palladium catalysts for the Suzuki–Miyaura cross-coupling [16] and Mizoroki–Heck reaction [17] and heteronuclear complexes with lanthanides [18], octahedral nickel(II) complexes [19], copper(II) [20–23], scandium(III) [24], and cobalt(II) [25] complexes, as well as redox-active complexes with germanium(IV) [26]. Palladium(II) and chromium(III) complexes formed by azomethines containing heterocycles inhibit the growth of *S. marcescent*, *E. coli*, and *M. luteus* bacteria and possess a pronounced antitumor activity against MCF-7, HepG-2, and HCT-116 cancer cells [27]. Nickel(II) and platinum(II) complexes with bis-azomethine, 2-(5-(*tert*-butyl)-2-hydroxybenzylidene)-*N*-cyclohexylhydrazine-1-carbothioamide, exhibit a considerable antibacterial activity against *E. coli* and *S. aureus* [28]. Azomethine metal complexes are used to manufacture additives for lubricating compositions [29]. Zinc(II) azomethine complexes exhibit photoluminescent properties and fungicidal activity [30].

Changing the molecular geometry of azomethines may afford liquid crystals with optical properties [31] and smectic crystalline materials for manufacturing organic field-effect transistors [32].

Azomethines and their metal complexes possess luminescent properties. Shienok et al. [33] obtained azomethine with tetraarylimidazole moieties possessing tunable luminescence for molecular switches. Azomethines containing benzodifuran-thiophene moieties are used to fabricate optoelectronic devices [34]. Azomethines based on tris(2-aminoethyl)amine show emission in the 380–515 nm range in the solid-state and are promising as components of light-emitting diodes [35]. Azomethines with pyrazole groups show a large Stokes shift in tetrachloromethane, which allows them to be used in fluorescent molecular probes [36]. Zinc complexes of azomethine ligands, *N*,*N*-bis(salicylaldehyde)-2,3-diaminonaphthalene and *N*,*N*-bis(1-naphthalidimine)-2,3-diaminonaphthalene, act as light-emitting components in the development of fluorescent sensors and organic display devices [37].

The introduction of azomethine bonds into aminolysed polyethylene terephthalate is a new method for processing hazardous polymer wastes in order to obtain metal chelates [38].

Aryloxycyclophosphazenes containing azomethine groups are of particular research interest. They are widely used in biomedicine [39], as flame retardant materials [40], for coordination chemistry and catalysis [41], and as fluorescent dyes [42]. This is due to their polyfunctionality, biocompatibility, high thermal stability, flame resistance, and UV radiation resistance. Aslan F. et al. [43,44] synthesized several dozens of aryloxycyclophosphazenes with various substituents at the azomethine group formed by hexakis-[(4-formyl)phenoxy]cyclotriphosphazene and hexakis-[(2-formyl)phenoxy]cyclotriphosphazene. However, nothing was known about the crystal structure of azomethine derivatives. The main challenge was to obtain a single crystal. The single crystals of low-molecular-weight azomethines are often obtained by evaporation of the solvent from, for example, ethanol solutions [8]. In the case of the high-molecular-weight compounds of a complex architecture, most of the existing methods are inapplicable. Therefore, in this study, we tested a new method using specially synthesized hexakis-[4-{(N-allylimino)methyl}phenoxy]cyclotriphosphazene. Finally, we obtained a single crystal of this compound and studied it by X-ray diffraction.

2. Materials and Methods

2.1. Materials

Hexachlorocyclotriphosphazene, 99% (Fushimi Pharmaceutical Co., Ltd., Marugame, Kagawa Prefecture, Japan). 4-Hydroxybenzaldehyde, 98%; allylamine, 98%; magnesium sulfate, anhydrous, ≥99.5%; dichloromethane, ≥99.5%; chloroform, anhydrous, ≥99%; tetrahydrofuran, anhydrous, ≥99.9%; sodium, 99.9%; ethanol, anhydrous, ≥99.5%; toluene, anhydrous, 99.8%; hexane, anhydrous, 95% (Sigma-Aldrich, Saint Louis, MO, USA).

2.2. Methods

^{1}H, ^{13}C, and ^{31}P NMR spectra were recorded on an Agilent/Varian Inova 400 spectrometer (Agilent Technologies, Santa Clara, CA, USA) operating at 400.02 MHz, 100.60 MHz, and 161.94 MHz, respectively. MALDI-TOF mass spectrometry data were acquired using a Bruker Auto Flex II mass spectrometer (Bruker, Billerica, MA, USA). Differential scanning calorimetry (DSC) measurements were done using a NETZSCH STA 449F1 instrument (Erich NETZSCH GmbH & Co. Holding KG, Selb, Germany).

Crystallographic data: Crystals of APP ($C_{60}H_{60}N_9O_6P_3$, M = 1096.08) are monoclinic, space group $P2_1/n$; at 296 K: a = 8.4373(2), b = 14.9917(3), c = 46.2319(8) Å, β = 94.4940(10)°, V = 5829.9(2) Å^3, Z = 4, d_{calc} = 1.249 g cm^{-3}, μ(MoKα) = 1.60 cm^{-1}, and F(000) = 2304. The intensities of 66102 reflections were measured with a Bruker Quest D8 CMOS diffractometer (Bruker AXS, Madison, USA) [λ(MoKα) = 0.71073 Å, ω-scans, 2θ < 54°], and 12686 independent reflections were used for further refinement. Using Olex2 [45], the structure was solved with the ShelXT [46] structure solution program using Intrinsic Phasing and refined with the XL [46] refinement package using least-squares minimization. Hydrogen atom positions were calculated and refined in the isotropic approximation within

the riding model. The refinement converged to wR2 = 0.2024 and GOF = 1.097 for all the independent reflections (R1 = 0.0782 was calculated against F for 8108 observed reflections with I > 2σ(I)). CCDC 2174092 contains the supplementary crystallographic; information for this paper.

The size of the APP molecule was determined by processing X-ray diffraction data using Mercury 3.8 software (created by CCDC, CSD license).

2.3. Synthesis of Hexakis-[(4-formyl)phenoxy]cyclotriphosphazene (FPP)

Hexakis-[4-formylphenoxy]cyclotriphosphazene was synthesized by the procedure described in a previous study [47].

4-Hydroxybenzaldehyde (7.32 g, 0.06 mol) was dissolved in ethanol (30 mL) in a three-necked flask equipped with a stirrer and a reflux condenser. After complete dissolution of 4-hydroxybenzaldehyde, the alcohol solution of sodium ethylate, which was obtained via dissolution of sodium (1.15 g, 0.05 mol) in ethanol (20 mL), was loaded into the flask. The reaction time was 10 min. Then, ethanol was distilled off on a rotary evaporator in vacuum. The residue was dried in vacuum up to a constant weight. The yield of the product was quantitative.

4-Hydroxybenzaldehyde phenolate (8.64 g, 0.06 mol) was loaded in a three-necked flask equipped with a stirrer and a reflux condenser, and tetrahydrofuran (40 mL) was added. A solution of hexachlorocyclotriphosphazene (2.61 g, 0.0075 mol) in tetrahydrofuran (20 mL) was added to the dispersion formed during stirring. The time of reaction was 9 h during solvent boiling. When the process was complete, the reaction mixture was filtered off and the mother liquor was evaporated on a rotary evaporator. The product was recrystallized from the ethanol–chloroform mixture. Yield: 4.52 g (70%).

2.4. Synthesis of Hexakis-[4-{(N-allylimino)methyl}phenoxy]cyclotriphosphazene (APP)

Hexakis-[(4-formyl)phenoxy]cyclotriphosphazene (0.5 g, 0.5807 mmol) was charged into a 50 mL round-bottom flask and dissolved in dichloromethane (5 mL). After complete dissolution, allylamine (0.31 mL, 4.181 mmol) and magnesium sulfate (0.56 g, 4.646 mmol) were added. The reaction mixture was magnetically stirred for 48 h at 25 °C. The solution was decanted from magnesium sulfate, and dichloromethane was evaporated on a rotary evaporator. The product was dried in a drying oven under vacuum at 40 °C for 4 h. Yield: 0.57 g (90%). The product was recrystallized from a toluene–hexane solvent system.

3. Results and Discussion

The synthesis of APP was performed according to the scheme shown in Figure 1. The reaction was conducted in a non-polar solvent to facilitate the removal of water. Magnesium sulfate was used as the drying agent. A 20% molar excess of allylamine over aldehyde groups was used to ensure complete aldehyde to azomethine conversion.

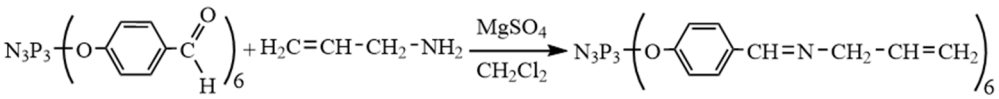

Figure 1. Synthesis of APP.

The excess allylamine was removed under vacuum at a temperature not higher than 40 °C, together with the solvent. In this case, the residue was a loose crystalline material. At higher temperature, an amorphous glassy material was formed, which later turned yellow as a result of side reactions.

The phosphorus NMR spectrum of the product is a singlet, indicating the absence of side reactions affecting the phosphazene ring (Figure 2B). This singlet is shifted by 1.7 ppm relative to the signal of the initial FPP (Figure 2A). This is caused by the difference between mesomeric effects of the aldehyde and azomethine groups affecting the phosphorous atoms of the phosphazene ring.

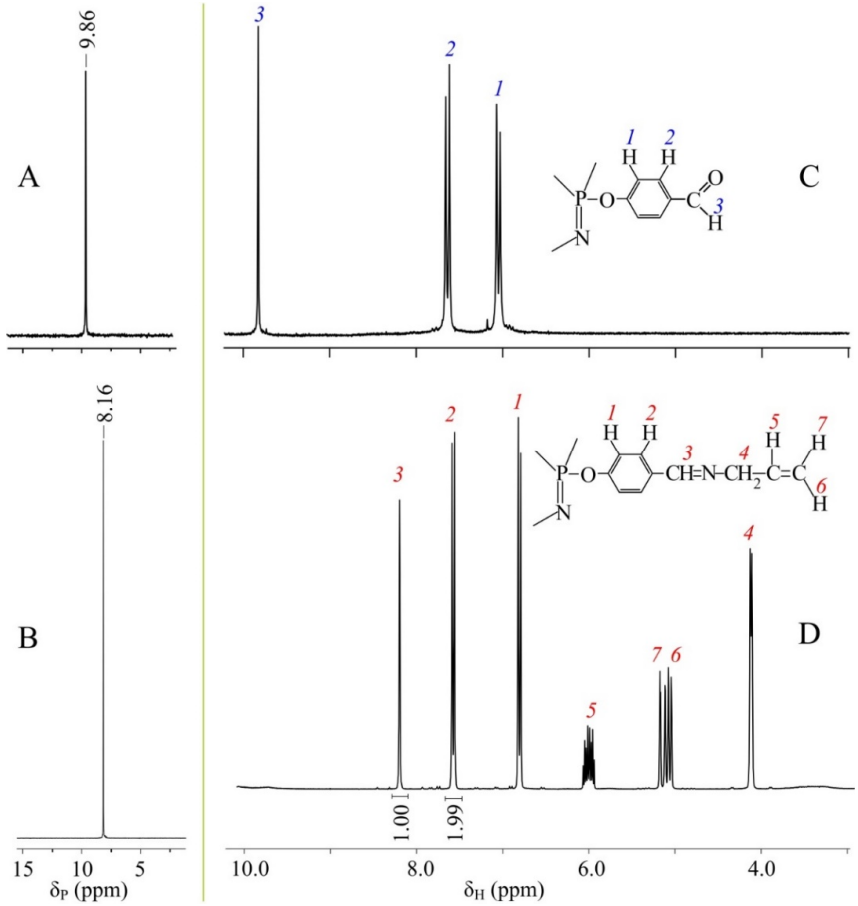

Figure 2. ^{31}P NMR spectra FPP (**A**) and APP (**B**) and ^{1}H NMR spectra of FPP (**C**) and APP (**D**).

A similar picture is observed for the ^{1}H NMR spectrum of the product (Figure 2D). The azomethine proton signal is shifted upfield by approximately 1.7 ppm relative to the proton signal of the aldehyde group (Figure 2C). The absence of a signal at 9.8 ppm in the spectrum of APP means that the aldehyde groups were completely converted to azomethine groups.

The completeness of the conversion is confirmed by ^{13}C NMR spectra (Figure 3A) and MALDI-TOF mass spectra (Figure 3B).

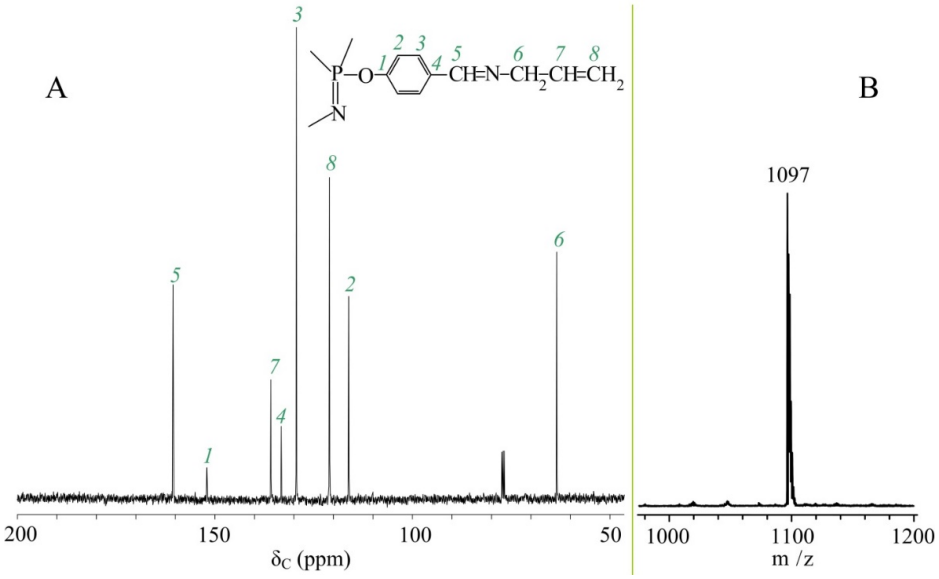

Figure 3. ^{13}C NMR spectra (**A**) and MALDI-TOF mass spectra (**B**) of APP.

The ^{13}C NMR spectrum shows a carbon signal for the azomethine group at 161 ppm, but no signal typical of the aldehyde group carbon at 191 ppm.

The MALDI-TOF mass spectrum has only one peak corresponding to the mass of the target product solvated by the matrix proton (1096 + H^+).

According to the DSC study of APP, the product was crystalline, but melted in a wide temperature range from 50 to 90 °C (Figure 4b). This attests to a polycrystalline structure with numerous defects.

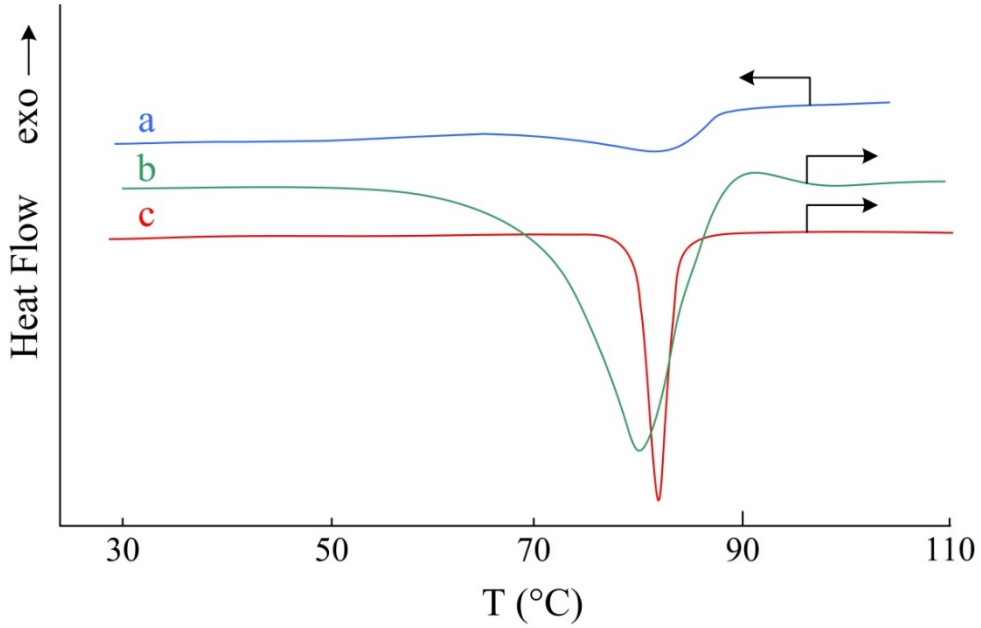

Figure 4. DSC curves of APP: heating before recrystallization (**b**) and after recrystallization (**c**) and cooling (**a**).

Considering the cooling curve shows that APP does not crystallize from the melt, since only a heat capacity step corresponding to the glass transition of the sample is observed. Hence, methods for the preparation of single crystals involving sample heating are inapplicable in this case. Methods of low-temperature evaporation of the solvent were also tested; however, with volatile solvents, crystallization took place rapidly and a single crystal was not formed. In the case of low-volatile solvents, crystallization was slow, but was accompanied by oxidation and yellowing of the compound. Therefore, we proposed an alternative method for the preparation of single crystals, which was based on the precipitation of the compound by the vapor of a volatile solvent from a solution in a low-volatile solvent in a confined space. The vessel in which crystallization took place was filled with an inert gas (argon). The method is based on the use of a closed system in which two liquids with different volatility are placed, separated by a partition. Accordingly, the filling of the volume with vapors of these liquids begins, while the volume is saturated with vapors of a more volatile liquid. Since the pressure of saturated vapor over a slightly volatile liquid is less than over a highly volatile liquid, slow diffusion of the vapors of a volatile liquid into a slightly volatile liquid occurs. If, however, a solution of a crystalline substance is prepared in a slightly volatile liquid and a highly volatile liquid is used in which the substance does not dissolve, the substance will be gradually displaced by vapors of the volatile liquid from the solution and form crystals (Figure 5).

In our case, toluene was chosen as a slightly volatile liquid in which a solution of APP was prepared. Hexane was chosen for precipitation as it is inert, readily dehydrated, and can dissolve the residual allylamine and dichloromethane. Deposition with hexane vapor led to the formation of relatively large hexagonal lamellar single crystals with an average face size of about 1 mm, suitable for X-ray diffraction studies.

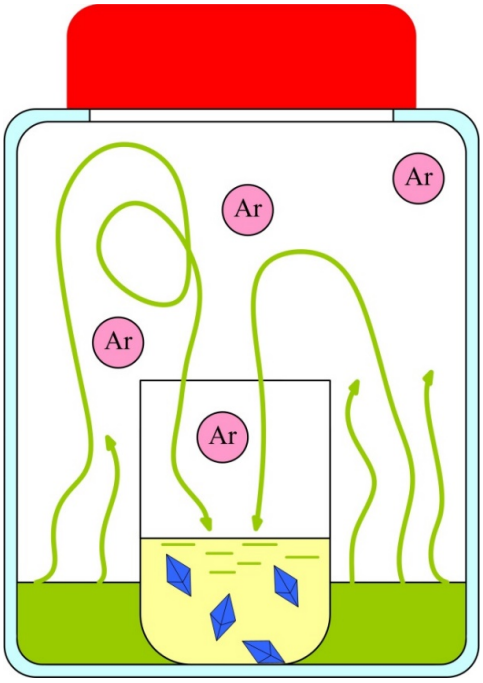

Figure 5. Crystallization in a confined space.

The DSC curve of the recrystallized and dried APP sample shows a melting peak in a narrow temperature range (Figure 4c) of 78–85 °C with a maximum at 82 °C, which indirectly confirms the ordering of the sample structure and the absence of defects.

The single crystals grown by the developed method were studied by X-ray diffraction (Figure 6). The X-ray diffraction data from a single crystal were collected at room temperature and accessed using no operational low-temperature device. At this temperature, the heterocyclic P_3N_3 core adopts a flattened chair conformation, with the atoms P(2) and N(3) deviating from the mean plane of the other atoms by 0.256(3) and 0.156(3) Å, respectively. The substituents reside at the phosphorus atoms in the axial positions on both sides of the P_3N_3 core. The phenyl rings of the neighboring substituents are rotated so that no intramolecular stacking interactions occur between them; the angles of the two such rings relative to the third one on the opposite sides of the P_3N_3 core are 29.25(13), 53.91(15) and 10.21(13), 56.88(13)°, respectively. The lack of intermolecular stacking interactions may arise from the bulky allyl groups that are severely disordered at the accessed temperature and thereby prevent the phenyl groups from approaching each other. As a result, the molecules of APP are held together only by weak van der Waals contacts. More detailed information about the APP structure is presented in the Supplementary Materials.

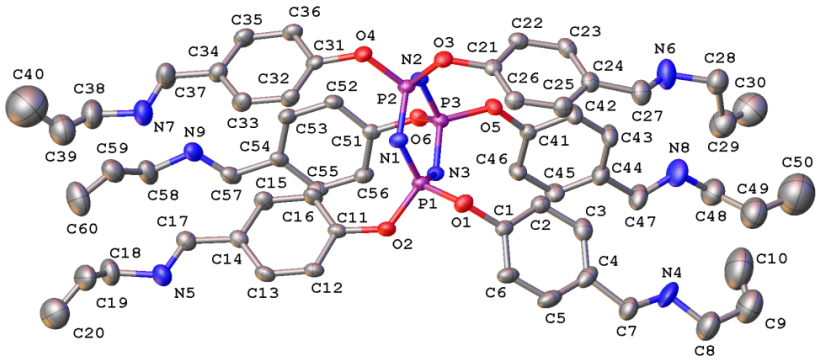

Figure 6. General view of the compound APP in the representation of non-hydrogen atoms as thermal ellipsoids at a 20% probability level. Hydrogen atoms as well as minor components of the disordered allyl groups are omitted for clarity.

It was shown that the sphere circumscribed around the APP macromolecule has a diameter of 2.382 nm, which allows assigning the molecule to nano-sized structures.

4. Conclusions

Thus, it can be concluded that the developed method for crystallization of macromolecules is applicable for the preparation of single crystals of high-molecular-weight (1096 Da) compounds with complex architecture. These macromolecules fall into the nanoscale range and can be used as nanoparticles in various fields of science and technology, for example, as modifying agents for polymer materials and as drug carriers, catalysts, chelators, and so on.

Supplementary Materials: The following supporting information can be downloaded at: https://www.mdpi.com/article/10.3390/nano12132268/s1, the files APP.cif and checkcif_APP.pdf with information about the APP structure are presented.

Author Contributions: Conceptualization, E.C.; methodology, E.C., P.Y., and Y.N.; validation, E.C.; formal analysis, E.C.; investigation, E.C., P.Y., and Y.N.; resources, E.C., P.Y., and Y.N.; data curation, E.C.; writing—original draft preparation, E.C., P.Y., and Y.N.; writing—review and editing, E.C.; visualization, E.C.; supervision, E.C.; project administration, E.C.; funding acquisition, E.C. All authors have read and agreed to the published version of the manuscript.

Funding: The survey was funded by the Russian Science Foundation grant No. 22-43-02056, https://rscf.ru/project/22-43-02056/ (accessed on 9 March 2022).

Acknowledgments: X-ray diffraction data were collected using the equipment of the Center for Molecular Composition studies of INEOS RAS with financial support from the Ministry of Science and Higher Education of the Russian Federation (Contract/agreement No. 075-00697-22-00).

Conflicts of Interest: The authors declare no conflict of interest.

References

1. Whitty-Léveillé, L.; Tremblay-Cantin, J.C.; Picard-Lafond, A.; Boudreau, D.; Reynier, N.; Larivière, D. Core-shell nanoparticles bearing Schiff base ligand for the selective extraction of uranium from REE leach liquors. *Hydrometallurgy* **2022**, *208*, 105780. [CrossRef]
2. Chang, I.J.; Choi, M.G.; Jeong, Y.A.; Lee, S.H.; Chang, S.K. Colorimetric determination of Cu2+ in simulated wastewater using naphthalimide-based Schiff base. *Tetrahedron Lett.* **2017**, *58*, 474–477. [CrossRef]
3. Taniguchi, T.; Urayama, K. Linear dynamic viscoelasticity of dual cross-link poly (vinyl alcohol) hydrogel with determined borate ion concentration. *Gels* **2021**, *7*, 71. [CrossRef] [PubMed]
4. Sánchez-Ponce, L.; Galindo-Riaño, M.D.; Casanueva-Marenco, M.J.; Granado-Castro, M.D.; Díaz-de-Alba, M. Sensing Cd (II) Using a Disposable Optical Sensor Based on a Schiff Base Immobilisation on a Polymer-Inclusion Membrane. Applications in Water and Art Paint Samples. *Polymers* **2021**, *13*, 4414. [CrossRef]
5. El-Hiti, G.A.; Ahmed, D.S.; Yousif, E.; Al-Khazrajy, O.S.; Abdallh, M.; Alanazi, S.A. Modifications of polymers through the addition of ultraviolet absorbers to reduce the aging effect of accelerated and natural irradiation. *Polymers* **2021**, *14*, 20. [CrossRef]
6. Hashim, N.Z.N.; Kahar, M.A.M.; Kassim, K.; Embong, Z. Experimental and theoretical studies of azomethines derived from benzylamine as corrosion inhibitors of mild steel in 1 M HCl. *J. Mol. Struct.* **2020**, *1222*, 128899. [CrossRef]
7. Hegazy, M.A.; Rashwan, S.M.; Meleek, S.; Kamel, M.M. Synthesis, characterization and mitigation action of innovative Schiff base on steel disintegration in sulfuric acid solution. *Mater. Chem. Phys.* **2021**, *267*, 124697. [CrossRef]
8. Abu-Yamin, A.A.; Jbarah, A.A.Q.M.; Al Khalyfeh, K.; Matar, S.A.; Alqasaimeh, M.; Rüffer, T.; Lang, H. Crystal structure, spectroscopic studies, DFT calculations, and biological activity of 5-bromosalicylaldehyde–based Schiff bases. *J. Mol. Struct.* **2022**, *1262*, 132976. [CrossRef]
9. Restrepo-Acevedo, A.; Osorio, N.; Giraldo-López, L.E.; D'Vries, R.F.; Zacchino, S.; Abonia, R.; Le Lagadec, R.; Cuenú-Cabezas, F. Synthesis and antifungal activity of nitrophenyl-pyrazole substituted Schiff bases. *J. Mol. Struct.* **2022**, *1253*, 132289. [CrossRef]
10. Ermiş, E.; Durmuş, K. Novel thiophene-benzothiazole derivative azomethine and amine compounds: Microwave assisted synthesis, spectroscopic characterization, solvent effects on UV–Vis absorption and DFT studies. *J. Mol. Struct.* **2020**, *1217*, 128354. [CrossRef]
11. Zheng, J.; Yu, Y.; Zhen, X.; Yang, E.; Zhao, Y. Synthesis and Characterization of Nitrogen Heterocyclic Derivatives Containing Sulfur–Ether and Schiff Base. *Phosphorus Sulfur Silicon Relat. Elem.* **2013**, *188*, 1564–1575. [CrossRef]
12. Korkmaz, A.; Bursal, E. Benzothiazole sulfonate derivatives bearing azomethine: Synthesis, characterization, enzyme inhibition, and molecular docking study. *J. Mol. Struct.* **2022**, *1257*, 132641. [CrossRef]

13. Vildanova, R.; Lobov, A.; Spirikhin, L.; Kolesov, S. Hydrogels on the Base of Modified Chitosan and Hyaluronic Acid Mix as Polymer Matrices for Cytostatics Delivery. *Gels* **2022**, *8*, 104. [CrossRef] [PubMed]
14. Donia, A.M.; Atia, A.A.; Elwakeel, K.Z. Recovery of gold (III) and silver (I) on a chemically modified chitosan with magnetic properties. *Hydrometallurgy* **2007**, *87*, 197–206. [CrossRef]
15. Pudovik, M.A.; Kibardina, L.; Trifonov, A.; Dobrynin, A.; Katsyuba, S.; Burilov, A. Phosphorylation of pyridoxal azomethines. Synthesis of phosphorus containing azomethines and furopyridines. *Phosphorus Sulfur Silicon Relat. Elem.* **2019**, *194*, 120–126. [CrossRef]
16. Sünbül, A.B.; Inan, A.; Köse, M.; Evren, E.; Gürbüz, N.; Ozdemir, İ.; Ikiz, M.; Dag, A.K.; Ispir, E. Azo-azomethine based palladium (II) complexes as catalysts for the Suzuki-Miyaura cross-coupling reaction. *J. Mol. Struct.* **2020**, *1216*, 128279. [CrossRef]
17. Vibhute, S.P.; Mhaldar, P.M.; Shejwal, R.V.; Rashinkar, G.S.; Pore, D.M. Palladium Schiff base complex immobilized on magnetic nanoparticles: An efficient and recyclable catalyst for Mizoroki and Matsuda-Heck coupling. *Tetrahedron Lett.* **2020**, *61*, 151801. [CrossRef]
18. Osypiuk, D.; Cristóvão, B.; Mazur, L. New heteronuclear complexes of PdII–LnIII–PdII with Schiff base ligand: Synthesis, crystal structures and chemical properties. *J. Mol. Struct.* **2022**, *1261*, 132924. [CrossRef]
19. Dehghani-Firouzabadi, A.A.; Morovati, F.; Notash, B. Metal complexes with thioether containing unsymmetrical Ni2S donor Schiff base ligand: Crystal and molecular structure of nickel (II) complex. *Phosphorus Sulfur Relat. Elem.* **2020**, *195*, 644–650. [CrossRef]
20. Burlov, A.S.; Lyssenko, K.A.; Koshchienko, Y.V.; Nikolaevskii, S.A.; Vasilchenko, I.S.; Garnovskii, D.A.; Uraev, A.I.; Garnovskii, A.D. Mixed-ligand azomethine–benzimidazole palladium complex. *Mendeleev Commun.* **2008**, *4*, 198–199. [CrossRef]
21. Bazhin, D.N.; Kudyakova, Y.S.; Slepukhin, P.A.; Burgart, Y.V.; Malysheva, N.N.; Kozitsina, A.N.; Ivanova, A.V.; Bogomyakov, A.S.; Saloutin, V.I. Dinuclear copper (ii) complex with novel N, N′, N″, O-tetradentate Schiff base ligand containing trifluoromethylpyrazole and hydrazone moieties. *Mendeleev Commun.* **2018**, *28*, 202–204. [CrossRef]
22. Uraev, A.I.; Popov, L.D.; Levchenkov, S.I.; Shcherbakov, I.N.; Suponitsky, K.Y.; Garnovskii, D.A.; Lukov, V.V.; Kogan, V.A. Crystal structure and magnetic properties of a tetranuclear carbonate-bridged CuII complex with a Schiff base compartmental ligand with the N2OS2 donor set. *Mendeleev Commun.* **2015**, *25*, 62–64. [CrossRef]
23. Yek, S.M.G.; Nasrollahzadeh, M.; Azarifar, D.; Rostami-Vartooni, A.; Ghaemi, M.; Shokouhimehr, M. Grafting Schiff base Cu (II) complex on magnetic graphene oxide as an efficient recyclable catalyst for the synthesis of 4H-pyrano [2, 3-b] pyridine-3-carboxylate derivatives. *Mater. Chem. Phys.* **2022**, *284*, 126053.
24. Gurina, G.A.; Kissel, A.A.; Ob'edkov, A.M.; Cherkasov, A.V.; Trifonov, A.A. Alkyl scandium complexes coordinated by dianionic O, N, N-and O, N, O-ligands derived from Schiff bases. *Mendeleev Commun.* **2021**, *31*, 631–634. [CrossRef]
25. Borisova, N.E.; Ustynyuk, Y.A.; Reshetova, M.D.; Aleksandrov, G.G.; Eremenko, I.L.; Moiseev, I.I. New polydentate Schiff bases and their cobalt complexes. *Mendeleev Commun.* **2003**, *13*, 202–204. [CrossRef]
26. Krylova, I.V.; Saverina, E.A.; Rynin, S.S.; Lalov, A.V.; Minyaev, M.E.; Nikolaevskaya, E.N.; Syroeshkin, M.A.; Egorov, M.P. Synthesis, characterization and redox properties of Ar–C= N→ Ge← N= C–Ar containing system. *Mendeleev Commun.* **2020**, *30*, 563–566. [CrossRef]
27. Aljohani, F.S.; Abu-Dief, A.M.; El-Khatib, R.M.; Al-Abdulkarim, H.A.; Alharbi, A.; Mahran, A.; Khalifa, M.E.; El-Metwaly, N.M. Structural inspection for novel Pd (II), VO (II), Zn (II) and Cr (III)-azomethine metal chelates: DNA interaction, biological screening and theoretical treatments. *J. Mol. Struct.* **2021**, *1246*, 131139. [CrossRef]
28. Arafath, M.A.; Adam, F.; Hassan, M.Z. Synthesis, characterization, X-ray crystal structure and antibacterial activity of nickel, palladium and platinum complexes with Schiff base derived from N-cyclohexylhydrazinecarbothioamide and 5-(tert-butyl)-2-hydroxybenzaldehyde. *Phosphorus Sulfur Silicon Relat. Elem.* **2021**, *196*, 530–537. [CrossRef]
29. Garnovskii, A.D.; Ponomarenko, A.G.; Burlov, A.S.; Bicherov, A.V.; Konoplev, B.G.; Ageev, O.A.; Kolomiitsev, A.S.; Chetverikova, V.A.; Borodkina, I.G.; Chigarenko, G.G.; et al. Tribologically active azomethine metal complexes. *Russ. J. Gen. Chem.* **2010**, *80*, 982–986. [CrossRef]
30. Milutka, M.S.; Burlov, A.S.; Vlasenko, V.G.; Koshchienko, Y.V.; Makarova, N.I.; Metelitsa, A.V.; Korshunova, E.V.; Trigub, A.L.; Zubenko, A.A.; Klimenko, A.I. Synthesis, Structure, Spectral-Luminescent Properties, and Biological Activity of Chlorine-Substituted Azomethines and Their Zinc (II) Complexes. *Russ. J. Gen. Chem.* **2021**, *91*, 1706–1716. [CrossRef]
31. Alamro, F.S.; Ahmed, H.A.; Bedowr, N.S.; Khushaim, M.S.; El-Atawy, M.A. New Advanced Liquid Crystalline Materials Bearing Bis-Azomethine as Central Spacer. *Polymers* **2022**, *14*, 1256. [CrossRef] [PubMed]
32. Cozan, V.; Ardeleanu, R.; Airinei, A.; Timpu, D. Crystalline smectic E phase revisited in case of symmetrical dibenzo-18-crown-6-ether azomethine dimers. *J. Mol. Struct.* **2018**, *1156*, 22–29. [CrossRef]
33. Shienok, A.I.; Krutius, O.N.; Mardaleishvili, I.R.; Kol'tsova, L.S.; Popov, L.D.; Shepelenko, E.N.; Zaichenko, N.L. Synthesis and Spectral-Luminescent Properties of Fluorescent Dyads Based on Tetraarylimidazole and Azomethines of Various Nature. *Russ. J. Gen. Chem.* **2021**, *91*, 2101–2109. [CrossRef]
34. Moussallem, C.; Gohier, F.; Frère, P. Extended benzodifuran–thiophene systems connected with azomethine junctions: Synthesis and electronic properties. *Tetrahedron Lett.* **2015**, *56*, 5116–5119. [CrossRef]

35. Sęk, D.; Szlapa-Kula, A.; Siwy, M.; Fabiańczyk, A.; Janeczek, H.; Szalkowski, M.; Mackowski, S.; Schab-Balcerzak, E. Branched azomethines based on tris (2-aminoethyl) amine: Impact of imine core functionalization on thermal, electrochemical and luminescence properties. *Mater. Chem. Phys.* **2020**, *240*, 122246. [CrossRef]
36. Alam, M.S.; Lee, D.U. Molecular structure, spectral (FT-IR, FT-Raman, Uv-Vis, and fluorescent) properties and quantum chemical analyses of azomethine derivative of 4-aminoantipyrine. *J. Mol. Struct.* **2020**, *1227*, 129512. [CrossRef]
37. Gondia, N.K.; Sharma, S.K. Comparative optical studies of naphthalenebased Schiff base complexes for colour tunable application. *Mater. Chem. Phys.* **2019**, *224*, 314–319. [CrossRef]
38. Otaibi, A.A.A.; Alsukaibi, A.K.D.; Rahman, M.A.; Mushtaque, M.; Haque, A. From waste to Schiff base: Upcycling of aminolysed poly (ethylene terephthalate) product. *Polymers* **2022**, *14*, 1861. [CrossRef]
39. Chelike, D.K.; Alagumalai, A.; Acharya, J.; Kumar, P.; Sarkar, K.; Thangavelu, S.A.G.; Chandrasekhar, V. Functionalized iron oxide nanoparticles conjugate of multi-anchored Schiff's base inorganic heterocyclic pendant groups: Cytotoxicity studies. *Appl. Surf. Sci.* **2020**, *501*, 143963. [CrossRef]
40. DoĞan, S.; TÜmay, S.O.; Balci, C.M.; YeŞİlot, S.; BeŞlİ, S. Synthesis of new cyclotriphosphazene derivatives bearing Schiff bases and their thermal and absorbance properties. *Turk. J. Chem.* **2020**, *44*, 31. [CrossRef]
41. Doğan, S.; Balcı, C.M.; Şenocak, A.; Beşli, S. Cu (II) complexes of cyclotriphosphazene bearing Schiff bases: Synthesis, structural characterization, DFT calculations, absorbance and thermal properties. *Polyhedron* **2020**, *183*, 114541. [CrossRef]
42. İbişoğlu, H.; Ün, Ş.Ş.; Erdemir, E.; Tümay, S.O. Synthesis, characterization, and photophysical properties of cyclotriphosphazenes containing quinoline-4-aldehyde-p-oxyanil moieties. *Phosphorus Sulfur Silicon Relat. Elem.* **2021**, *196*, 760–768. [CrossRef]
43. Aslan, F.; Öztürk, A.İ.; Söylemez, B. Synthesis of fluorescence organocyclotriphosphazene derivatives having functional groups such as formyl, Schiff base and both formyl and Schiff base without using Ar or N2 atmosphere. *J. Mol. Struct.* **2017**, *1137*, 387–395. [CrossRef]
44. Aslan, F.; Demirpence, Z.; Tatsiz, R.; Turkmen, H.; Ozturk, A.I.; Arslan, M. The synthesis, characterization and photophysical properties of some new cyclotriphosphazene derivatives bearing Schiff base. *Z. Anorg. Allg. Chem.* **2008**, *634*, 1140–1144. [CrossRef]
45. Dolomanov, O.V.; Bourhis, L.J.; Gildea, R.J.; Howard, J.A.K.; Puschmann, H. OLEX2: A complete structure solution, refinement and analysis program. *J. Appl. Cryst.* **2009**, *42*, 339–341. [CrossRef]
46. Sheldrick, G.M. SHELXT—Integrated space-group and crystal-structure determination. *Acta Cryst. A* **2015**, *71*, 3–8. [CrossRef]
47. Chistyakov, E.M.; Kireev, V.V.; Filatov, S.N.; Terekhov, I.V.; Buzin, M.I.; Komarova, L.I. Thermal polycondensation of hexa-p-hydroxymethylphenoxycyclotriphosphazene. *Polym. Sci. Ser. B* **2012**, *54*, 407–412. [CrossRef]